DOI: 10.1002/cmdc.200500018

Discovery and Structure–Activity Relationship Studies of a Unique Class of HIV-1 Integrase Inhibitors

Raveendra Dayam, Tino Sanchez, and Nouri Neamati*[a]

HIV-1 integrase (IN) is an essential enzyme for viral replication and a validated target for the development of drugs against AIDS. Currently there are no approved drugs that target IN. However, new IN inhibitors are under clinical investigation. As more IN inhibitors enter human drug trials, there is a growing need for the design of novel lead compounds with diverse structural scaffolds and promising pharmacokinetic properties to counteract the difficulties observed with first-generation IN inhibitors. We have identified a novel class of IN inhibitors through the systematic exploration of structure–activity relationships in a series of linomide analogues. The predicted bound conformation of the most active analogues inside the IN active site also supports the observed structure–activity correlation in this new compound class.

Introduction

HIV-1 reverse transcriptase (RT), integrase (IN), and protease (PR) are virally encoded enzymes essential for viral replication process. Currently, 19 FDA-approved inhibitors of RT, PR, and the viral entry process are available for HIV/AIDS therapy. Highly active anti-retroviral therapy, which involves the combination of these drugs, drastically decreases viral spread and provides a significant improvement in the life expectancy of HIV/AIDS patients. However, the rapid emergence and spread of drug-resistant HIV-1 strains and serious long-term toxic effects of available anti-retroviral drugs has generated demand for the design of new drugs with novel mechanisms of action, targeting critical steps in the retroviral replication processes.[1–3] HIV-1 IN mediates an obligatory step in the viral replication process by catalyzing the integration of viral cDNA into the host genome.[4] Therefore, the inhibition of IN catalytic activities offers a promising anti-retroviral drug target. IN mediates the integration process in two steps. In the first step, IN cleaves two terminal nucleotides from the conserved 3′ ends of the viral DNA in the cytoplasm of the infected cell. This step is called 3′ processing. IN carries the processed viral cDNA into the nucleus as a part of the pre-integration complex. In the second step, IN mediates integration of the processed viral cDNA into the host genome. This step is known as the strand-transfer process. Previously several IN inhibitors were identified through in vitro inhibition assays with recombinant IN.[5,6] Among all the reported inhibitors, the β-diketo acid class of compounds showed the most promising results.[7,8] S-1360 (**1**) and L-870,810 (**2**) represent the first generation of IN inhibitors that have entered clinical studies (Figure 1).[9,10]

Unlike RT and PR, limited structural information on IN interaction with inhibitors has been published.[11] A crystal structure of the IN core domain complexed with the β-diketo acid bioisostere 5CITEP (**3**) is available.[12] Much of the progress in the discovery of IN inhibitors has been made through high-throughput screening and ligand-based computer-aided drug-design methods. Analogue and structure-based pharmacophore modeling provided several structurally diverse lead compounds.[13–20] Herein, we report the discovery of a novel class of IN inhibitors. This is the first report of an extensive structure–activity relationship (SAR) study on this class of compounds for the selection of candidate derivatives for detailed biological investigations.

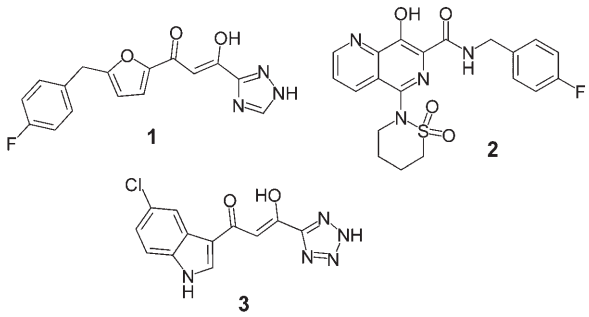

Figure 1. HIV-1 IN inhibitors S-1360 (**1**) and L-870,810 (**2**) in clinical trials; 5CITEP (**3**) was co-crystallized with the IN core domain to provide the first crystallographically determined structure of HIV-1 IN complexed with an inhibitor.

Results and Discussion

Recently, we identified the lead compound **4** as part of a study to discover structurally diverse IN inhibitors with novel structural scaffolds and which are readily amenable to structural modifications (Figure 2, manuscript under review). The lead

[a] *R. Dayam, T. Sanchez, Prof. N. Neamati*
Department of Pharmaceutical Sciences
University of Southern California, School of Pharmacy
1985 Zonal Avenue, Los Angeles, California 90089 (USA)
Fax: (+1) 323-442-1390
E-mail: neamati@usc.edu

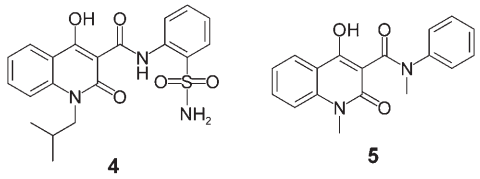

Figure 2. Lead compound **4** and roquinimex (**5**).

compound **4** was retrieved from a database of approximately 150,000 molecules by using a common-feature 3D pharmacophore model. Compound **4** inhibited both 3′ processing and strand-transfer activities of IN with IC_{50} values of 40 ± 3 and 16 ± 6 μM, respectively. The mapping of the common-feature pharmacophore model (Hypo 1) onto compound **4** shows reasonable agreement between pharmacophore features and chemical features (Figure 3). With a novel structural scaffold,

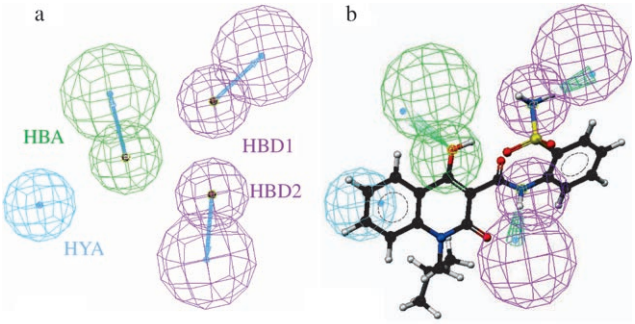

Figure 3. a) Common feature pharmacophore (Hypo 1) model used to retrieve lead compound **4** from the database; the pharmacophore features are shown as hydrophobic (HYA) in blue, H-bond acceptor (HBA) in green, and H-bond donor (HBD1, 2) in magenta. b) The mapping of lead compound **4** onto the pharmacophore model shows a reasonable agreement between pharmacophore features and the chemical features of the compound **4**.

compound **4** represents a new class of IN inhibitors. It is interesting to note that compound **4** can adopt a conformation that is similar to that of the diketo or keto–enol arrangement observed in compounds **1**–**3**. Considering the structural novelty of **4**, we carried out an extensive SAR study to select a compound for future cell-based studies. Furthermore, compound **4** is a close analogue of roquinimex (**5**), a previously reported anti-neoplastic agent (Figure 2). Roquinimex (**5**), also known as linomide, has strong immunomodulatory effects in animals and humans.[21,22] Interestingly, roquinimex suppressed HIV-1 infection in SCID-hu-PBL mice by promoting an increase in human CD4+ T-cell counts.[23] This activity was attributed to its immunomodulatory effects. Several analogues of roquinimex were also evaluated for the treatment of autoimmune disorders.[24] Therefore, on the basis of these previously reported biological properties of roquinimex and its analogues and our reported IN inhibitory activity of compound **4**, a detailed SAR study was warranted.

A set of over 150 analogues was retrieved from the database using the core substructure of compound **4**, which is shown in Figure 4. We tested compounds **6**–**23** (Table 1) to explore the influence toward IN inhibitory activity of the size of the hydrophobic substitution R^1 on N1 of the quinolinone-3-carboxamide core as well as substitutions R^2 and R^3 on the phenyl group of the *N*-carboxamide group. Analogues **6**–**15** are reasonably mapped by pharmacophore features of Hypo 1. Interestingly, most compounds from this set except compounds **7**, **14**, and **15** inhibited both the 3′ processing and strand-transfer activities of IN with IC_{50} values <100 μM. Indeed, this set of compounds represents the most active analogues of compound **4** that have been identified so far. The size and shape of the hydrophobic substitution R^1 on N1 of the quinolinone-3-carboxamide core plays an important role in the IN inhibitory activity of this set of compounds. The inhibitory potency of the compounds increases with increasing aliphatic chain size (compounds **4**, **6**, **8**–**10**, and **13**). The most active compounds, **10** and **13**, possess an *n*-pentyl chain, whereas the *n*-hexyl functionalized compound **15** is inactive. It appears that the *n*-pentyl chain length is optimal and required for potency against IN. The activity profile of compounds **6**–**15** suggests that the presence of a group containing both H-bond acceptor and donor properties at the R^2 position is an important requirement for the compound to be active against IN. However, the presence of a group that has only H-bond donor properties allows the compound to be mapped by Hypo 1 (such as the $-NH_2$ group in compound **14**), but it does not make the compound active against IN. The IN inhibitory activity of compounds **17**–**19** supports this observation. Compounds that have an H-bond acceptor group at the R^2 position selectively inhibit the strand-transfer activity of IN. The most potent member of this set, compound **17**, has 10-fold selectivity toward inhibition of the strand-transfer reaction over inhibition of the 3′ processing reaction of IN. Compound **17**, equipped with a methyl acetate group at the R^2 position, inhibited the 3′ processing and strand-transfer activities of IN with IC_{50} values of 100 and 9.5 μM, respectively. Furthermore, the predicted bound conformation of compound **13** inside the IN active site also supports this observation. The hydroxy group (at the R^2 position) of compound **13** forms H-bond interactions with the carboxylate oxygen atoms of amino acid residue D64 and also chelates the active site Mg^{2+} ion (see below). This indicates that a hydrogen-bond accepting group at the R^2 position is an essential requirement for inhibitory activity (through Mg^{2+} chelation) and confers selectivity toward the strand-transfer reaction of IN (see compounds **17**–**19**, Table 1).

The observed inactivity of the compounds in which $R^1=n$-hexyl (compounds **21** and **22**), and in which $R^2=Cl$ (compound

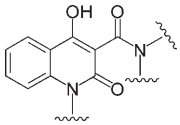

Figure 4. The core substructure of compound **4** used to retrieve analogues from the database.

Table 1. HIV-1 IN inhibitory activity of lead compound **4** analogues **6**–**23**.

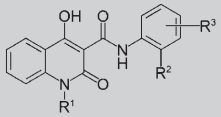

Compd	Structure			IC_{50} [μM]	
	R^1	R^2	R^3	3′ Processing	Strand Transfer
4	$CH_2CH(CH_3)_2$	SO_2NH_2	H	40 ± 3	16 ± 6
6	CH_3	SO_2NH_2	H	50 ± 6	39 ± 6
7	CH_2CH_3	SO_2NH_2	H	> 100	> 100
8	$CH_2CH{=}CH_2$	SO_2NH_2	H	83 ± 16	45 ± 5
9	$CH_2(CH_2)_2CH_3$	SO_2NH_2	H	15 ± 5	17 ± 5
10	$CH_2(CH_2)_3CH_3$	SO_2NH_2	H	11 ± 5	13 ± 4
11	CH_3	OH	4-NO_2	> 100	> 100
12	CH_2CH_3	OH	H	72 ± 18	32 ± 1
13	$CH_2(CH_2)_3CH_3$	OH	5-NO_2	9 ± 5	9 ± 4
14	$CH_2CH_2CH_3$	NH_2	H	> 100	> 100
15	$CH_2(CH_2)_4CH_3$	$CONH_2$	H	> 100	> 100
16	H	H	4-OH	> 100	> 100
17	CH_2CH_3	$COOCH_3$	H	100	9
18	$CH_2CH{=}CH_2$	OCH_3	H	> 100	25
19	CH_2CH_3	OCH_3	5-Cl	74 ± 36	19 ± 8
20	CH_3	CF_3	H	81 ± 18	28 ± 11
21	$CH_2(CH_2)_3CH_3$	Cl	H	> 100	> 100
22	$CH_2(CH_2)_3CH_3$	F	H	> 100	> 100
23	$CH_2(CH_2)_2CH_3$	H	H	> 100	> 100

21), F (compound **22**), or H (compound **23**) also supports the above-mentioned correlation between the IN inhibitory activity of the compound and the size of the hydrophobic group at R^1 and H-bonding properties of substituents at R^2. Moreover, it appears that the presence of a group with both H-bond accepting and donating properties at the R^2 position can turn a compound into a potent inhibitor but nonselective against IN catalytic reactions (such as compounds **13**, **10**, **9**, and **4**). Interestingly, a second substituent on the phenyl ring (at R^3) has no significant influence on IN inhibitory activity. However, a small to medium size substitution at the 5 position (compounds **19** and **13**) is better tolerated than is the same substitution at the 4 position of the phenyl ring (compound **11**). Compound **7**, with an ethyl group at the R^1 position and a sulfonamide group at R^2, was inactive at the maximum concentration tested of 100 μM.

Compounds **24**–**40** were also tested in the in vitro IN assay to explore the role of heterocyclic aromatic groups (with an H-bond acceptor heteroatom) or aliphatic groups on the carboxamide nitrogen atom in combination with a variety of aliphatic or aromatic hydrophobic groups on N1 of the quinolinone-3-carboxamide core of compound **4** (Table 2). Most of these compounds, equipped with a variety of heterocyclic aromatic or cyclic aliphatic groups such as pyridine, pyrimidine, thiazole, benzothiazole, furan, piperidine, cycloheptane, or adamantane on the carboxamide nitrogen atom with an aliphatic chain on N1 of the quinolinone-3-carboxamide core, were inactive at the maximum concentration tested (100 μM). Interestingly, many of these compounds, with at least a H-bond-accepting heteroatom (N, S, or O) at positions 2 or 5 on the heterocyclic aromatic group and an optimally sized aliphatic chain on N1 of the quinolinone-3-carboxamide core, failed to inhibit IN catalytic activity (compounds **24**, **26**–**30**, **36,** and **37**). Compound **25**, which has a 3-hydroxypyridine group and a cyclic aliphatic group on N1 to form a third ring on the quinolinone-3-carboxamide core, inhibited the 3′ processing and strand-transfer activities of IN with IC_{50} values of 56 and 15 μM, respectively. Further, the IN inhibitory activity of compound **25** supports the SAR observed in compounds from Table 1. Interestingly, compound **33**, which contains a thiadiazole group on the carboxamide nitrogen atom and a benzyl group on N1 of the quinolinone-3-carboxamide core, showed moderate IN inhibitory activity by blocking the 3′ processing and strand-transfer activities with IC_{50} values of 100 and 36 μM, respectively. Compound **39**, which has a 2-chlorobenzoyl group on the quinolinone-3-carbohydrazide core, showed moderate IN inhibitory activity with IC_{50} values for 3′ processing and strand transfer of 28 and 26 μM, respectively. The activity profile of the compounds shown in Table 2 demonstrates that the presence of an H-bond-acceptor heteroatom at the 2 or 5 positions on the heterocyclic aromatic group of the quinolinecarboxamide core is not sufficient to inhibit IN catalytic activity. The inhibitory activity of compound **25** underscores the importance of an aromatic or heterocyclic group functionalized with either H-bond acceptor or both H-bond acceptor and donor properties at *ortho* positions on the quinolinecarboxamide core (on the carboxamide nitrogen atom).

Compounds **41**–**47** were selected to determine the capacity of the quinolinone-3-carboxamide core of compound **4** alone to block the catalytic activities of IN (Table 3). These compounds were inactive at the maximum tested concentration of 100 μM. This confirms that the quinolinone-3-carboxamide core alone is insufficient for IN inhibitory activity. Furthermore, the lack of activity of compounds **44**–**47** against IN indicates the importance of an aromatic group that has suitable substitutions (such as H-bond acceptor groups) on the nitrogen atom of the carboxamide core, with respect to the analogues of compound **4**.

All compounds satisfied Lipinski's rule-of-five in the determination of calculated "druglike" properties. This rule was originally based on the analysis of 2245 compounds from the World Drug Index database in which it was found that approximately 90% of drugs marketed have the following features: 1) $M_r < 500$, 2) $\mathrm{Clog}\,P < 5$, 3) number of H-bond donors < 5 (sum of O–H and N–H), 4) number of H-bond acceptors < 10

Table 2. HIV-1 IN inhibitory activity of lead compound **4** analogues containing heterocyclic groups.

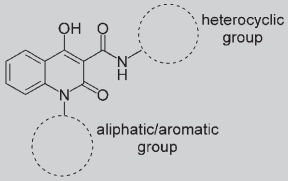

Compd	Structure		IC_{50} [μM]	
	Aliphatic/Aromatic Group	Heterocyclic Group	3′ Processing	Strand Transfer
24	$CH_2CH(CH_3)_2$		>100	>100
25	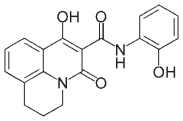		56±38	15±6
26	$CH_2(CH_2)CH_3$		>100	>100
27	$CH_2(CH_2)_3CH_3$		>100	>100
28	$CH_2(CH_2)_3CH_3$		>100	>100
29	$CH_2(CH_2)_3CH_3$	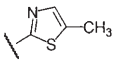	>100	>100
30	$CH_2(CH_2)_2CH_3$	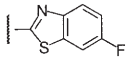	>100	>100
31	$CH_2(CH_2)_4CH_3$	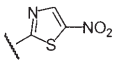	>100	>100
32	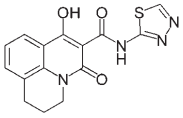		>100	>100
33			100	36
34	CH_3		>100	>100
35	$(CH_2)_2CH(CH_3)_2$		>100	>100
36	$CH_2(CH_2)_3CH_3$		>100	>100
37	$(CH_2)_2CH(CH_3)_2$		>100	>100
38	CH_2CH_3	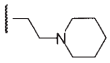	>100	>100
39	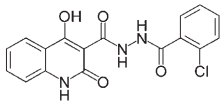		28	26
40	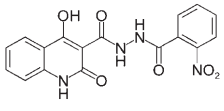		>100	>100

(sum of N and O atoms).[25,26] In addition to Lipinski's rule-of-five, we routinely calculate polar surface area (PSA) for all lead compounds.[27] Previously it was recommended that a maximum PSA value of ≈120 Å^2 is ideal for compounds intended for oral absorption by passive diffusion.[28,29] Therefore, compounds with PSA > 140 Å^2 would tend to show poor (<10%) absorption, whereas compounds for which PSA < 60 Å^2 are predicted to show complete (>90%) absorption. Several variants of PSA calculations such as dynamic (PSA_d), topological (TPSA), and fast (fPSA) are incorporated in various software packages.[30,31] We used fPSA to predict absorption as described, and the data are presented in Table 4. All compounds showed fPSA values <140 Å^2 and Log *P* values <5.

Docking studies were carried out with the most potent compound **13** to explore its binding orientation and critical interactions with amino acid residues located in the IN active site. Compound **13** was docked onto the active site region of IN wherein 5CITEP (**3**) was bound to the IN core domain observed in the structure of the IN–5CITEP complex (PDB code: 1QS4).[12] Compound **13** binds within the 5CITEP binding site, but the binding orientation of compound **13** is very different from that of 5CITEP. The predicted bound conformation of compound **13** is shown alongside that of 5CITEP in Figure 5. Compound **13** occupies an area that is surrounded by amino acid residues D64, H67, E92, D116, I151, E152, N155, K156, and K159. The *n*-pentyl group of compound **13** is positioned into a hydrophobic cavity at the bottom of the IN active site surrounded by amino acid residues Q62, V77 and I151. Two H-bonding interactions are observed between the carboxylate oxygen atoms of amino acid residue D64 and the 2-hydroxy group of the phenyl moiety on the carboxamide nitrogen atom (two O–H···O interactions with bond lengths of 2.62 and 2.22 Å). The hydroxy oxygen atom is strongly coordinated to

Table 3. HIV-1 IN inhibitory activity of analogues of the core unit of lead compound **4**.

Compd	Structure	IC_{50} [μM] 3′ Processing	Strand Transfer
41	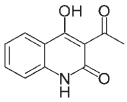	≫ 100	≫ 100
42	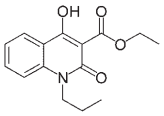	≫ 100	≫ 100
43	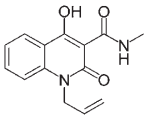	≫ 100	≫ 100
44	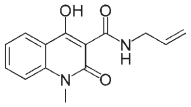	≫ 100	≫ 100
45	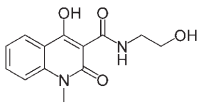	≫ 100	≫ 100
46	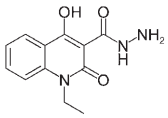	≫ 100	≫ 100
47	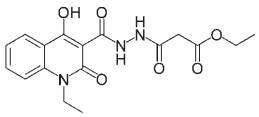	≫ 100	≫ 100

Table 4. Calculated druglike physicochemical properties of some of the active IN inhibitors.

Compd	M_r	Log $P^{[a]}$	No. H-Bond Acceptors	No. H-Bond Donors	No. Rotatable Bonds	fPSA [Å^2]
4	415.5	2.58	6	3	4	131.5
6	373.4	1.12	6	3	3	131.5
8	399.4	1.90	6	3	5	131.5
9	415.5	2.71	6	3	4	131.5
10	429.5	3.24	6	3	5	131.5
12	324.3	2.95	4	3	2	91.6
13	411.4	5.01	6	3	4	134.7
17	366.4	3.75	5	2	3	97.6
18	350.4	3.01	4	2	4	80.6
19	372.8	3.57	4	2	2	80.6
20	362.3	2.67	3	2	2	71.3
39	357.8	3.66	4	4	3	111.3

[a] Calculated atom-based Log *P*.

the Mg^{2+} ion (H–O···Mg^{2+} bond length: 1.77 Å). An additional H-bonding interaction is observed between the carboxamide NH group and the side chain hydroxy group of residue T66 (N–H···O–H bond length: 3.22 Å). The predicted bound conformation of compound **13** inside the IN active site strongly supports the coherent SAR observed in the analogues of compound **4**. Moreover, the bound conformation also reveals the importance of substitutions with H-bond acceptor and donor properties at the R^2 position and the critical role played by the size of the hydrophobic chain at the R^1 position toward the IN inhibitory activities of the active analogues of compound **4** (Table 1).

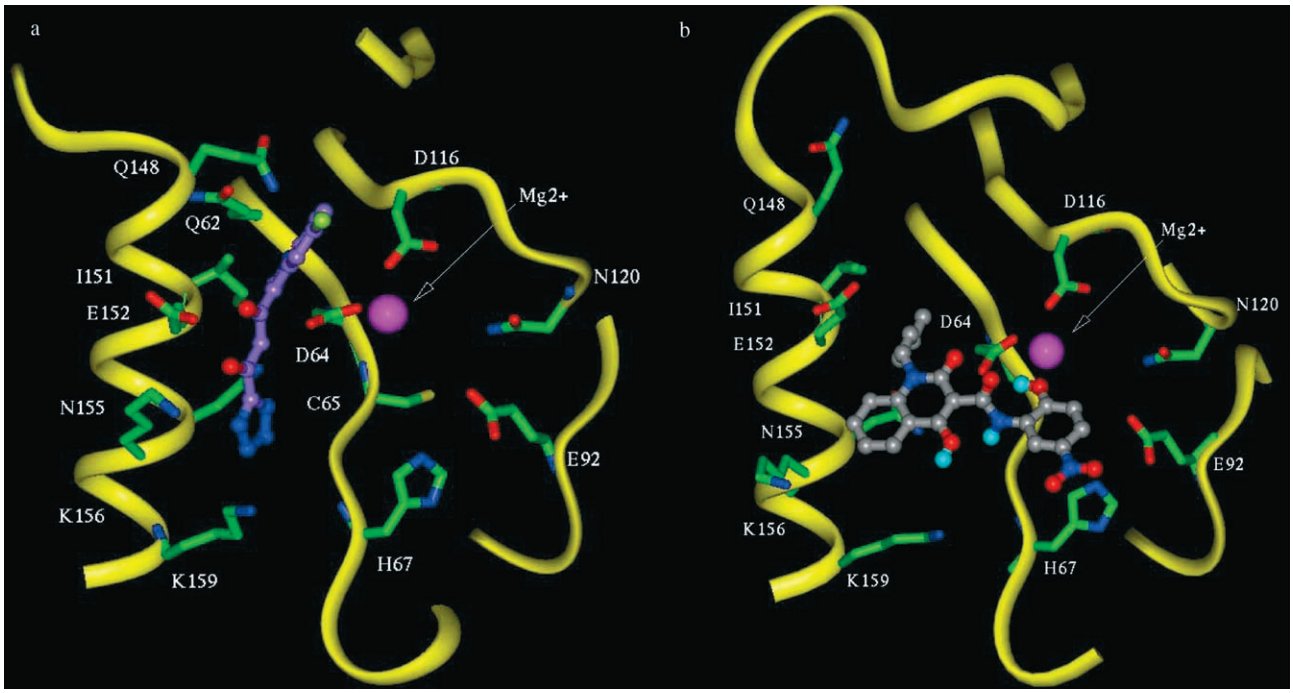

Figure 5. a) X-ray crystallographically determined bound conformation of 5CITEP (**3**) (ball-and-stick model in blue) inside the HIV-1 IN active site (PDB code: 1QS4). b) The predicted bound conformation of the most potent compound **13** (ball-and-stick model in gray) inside the IN active site. The ribbon model represents the active site region of IN, and the prominent amino acid residues are shown as stick models in green. The magenta sphere represents Mg^{2+}.

Conclusions

We have identified a novel class of IN inhibitors, performed a SAR study, and determined features important for activity. The predicted druglike properties of some of the active compounds make them potentially suitable candidates for further lead optimization in the effort to develop clinically useful IN inhibitors.

Materials and Methods

Selected compounds were purchased from Chemical Diversity, Inc., San Diego, CA, USA. All compounds were dissolved in DMSO, and the stock solutions were stored at −20 °C. γ-[^{32}P]-ATP was purchased either from Amersham Biosciences or ICN. The expression systems for the wild-type IN and soluble mutant IN F185K/C280S were generous gifts of Dr. Robert Craigie, Laboratory of Molecular Biology, NIDDK, NIH, Bethesda, MD, USA.

Oligonucleotide substrates: The oligonucleotides 21top (5′-GTGTGGAAAATCTCTAGCAGT-3′) and 21bot (5′-ACTGCTAGAGATTTTCCACAC-3′) were purchased from Norris Cancer Center Core Facility (University of Southern California) and purified by UV shadowing on polyacrylamide gel. To analyze the extent of 3′ processing and strand transfer with 5′-end labeled substrates, 21top was 5′-end labeled by using T_4 polynucleotide kinase (Epicentre, Madison, WI, USA) and γ-[^{32}P]-ATP. The kinase was heat-inactivated and 21bot was added in 1.5 molar excess. The mixture was heated at 95 °C, allowed to cool slowly to room temperature, and was run through a spi 25 mini-column (USA Scientific) to separate annealed double-stranded oligonucleotide from unincorporated material.

Integrase assays: To determine the extent of 3′ processing and strand transfer, wild-type IN was preincubated at a final concentration of 200 nM with the inhibitor in reaction buffer (NaCl (950 mM), HEPES (1 mM, pH 7.5), EDTA (50 μM), dithiothreitol (50 μM), glycerol (10%, *w/v*), $MnCl_2$ (7.5 mM), bovine serum albumin (0.1 mg mL^{-1}), 2-mercaptoethanol (10 mM), dimethyl sulfoxide (10%), and MOPS (25 mM, pH 7.2)) at 30 °C for 30 min. Then, the 5′-end ^{32}P-labeled linear oligonucleotide (20 nM) substrate was added, and incubation was continued for 1 h. Reactions were quenched by the addition of an equal volume (16 μL) of loading dye (deionized formamide (98%), EDTA (10 mM), xylene cyanol (0.025%), and bromophenol blue (0.025%)). An aliquot (5 μL) was electrophoresed on a denaturing polyacrylamide gel (tris–borate (0.09 M, pH 8.3), EDTA (2 mM), acrylamide (20%), urea (8 M)). Gels were dried, exposed in a PhosphorImager cassette, and analyzed with a Typhoon 8610 Variable Mode Imager (Amersham Biosciences) and quantified with ImageQuant 5.2 software. Percent inhibition (%*I*) was calculated with equation (1), in which *C*, *N*, and *D* are the fractions of 21-mer substrate converted into 19-mer (product of 3′ processing) or strand-transfer products for DNA alone, DNA plus IN, and IN plus drug, respectively. The IC_{50} values were determined by plotting the logarithm of drug concentration as a function of %*I* to identify concentrations at which 50% inhibition is observed.

$$\%I = 100 \times [1-(D-C)/(N-C)] \quad (1)$$

Docking studies: The subunit B of the core domain X-ray crystallographic structure of IN (PDB code: 1BIS), in which all active-site residues were resolved, was chosen for our docking experiment.[32] A Mg^{2+} ion was placed in the active site between the carboxylate oxygen atoms of residues D64 and D116 considering the geometry of the Mg^{2+} ion that is present in subunit A of IN (in PDB structure 1BIS) and subunit A of the IN–5CITEP complex (PDB structure 1SQ4).[12] All water molecules present in the protein were removed, and proper protonation states were assigned for acidic and basic residues of the protein. The most potent compound **13** was built and well-minimized with the Build module of the Insight II software package (Accelrys, Inc.).[33] Docking was performed with version 1.2 of the GOLD (Genetic Optimization for Ligand Docking) software package.[34] GOLD is an automated ligand-docking program that uses a genetic algorithm to explore the full range of ligand conformational flexibility with partial flexibility of the receptor.[35] The algorithm was tested on a dataset of over 300 complexes extracted from the Brookhaven Protein Data Bank.[36] GOLD succeeded in >70% cases in reproducing the experimentally determined bound conformation of the ligand. GOLD requires a user-defined binding site. It searches for a cavity within the defined area and considers all solvent-accessible atoms in the defined area as active-site atoms. An active site radius of 20 Å was defined with the carboxylate oxygen (OD1) atom of residue D64 as the center of the active site. Compound **13** was docked into the defined active site of IN. On the basis of the GOLD fitness score, a bound conformation with a high fitness score was considered as the best-bound conformation from a set of feasible bound conformations predicted by GOLD. All docking runs were carried out with standard default settings, a population size of 100, a maximum of 100000 operations, and a mutation and crossover rate of 95. The fitness function that was implemented in GOLD consisted basically of hydrogen bonding, complex energy, and ligand internal energy terms.

Computational ADMET analysis: Structures of all compounds were built and minimized in the Catalyst software package (Accelrys, Inc.). The possible unique conformations for each compound over an energy range of 20 kcal mol^{-1} were generated by using the best-conformation-generation method within the Catconf module of Catalyst. The low-energy conformers of all the compounds were exported to Accord (Accelrys, Inc.) to calculate Alogp98 and fast polar surface area (fPSA). The Log*P* values were also calculated with ADMET Predictor (Simulations Plus, Inc.).

Acknowledgements

This work was supported by funds from the Gustavus and Louise Pfeiffer Research Foundation and the GlaxoSmithKline Drug Discovery and Development Award to Nouri Neamati.

Keywords: antiviral agents · biological activity · drug design · pharmacophores · structure–activity relationships

[1] D. D. Richman, *Nature* **2001**, *410*, 995 – 1001.
[2] E. De Clercq, *Nat. Rev. Drug Discovery* **2002**, *1*, 13 – 25.
[3] E. De Clercq, *J. Med. Chem.* **2005**, *48*, 1297 – 1313.
[4] P. O. Brown (Ed.: J. J. Coffin, S. H. Hughes, H. E. Varmus), Cold Spring Harbor Press, NY, **1999**.
[5] R. Dayam, N. Neamati, *Curr. Pharm. Des.* **2003**, *9*, 1789 – 1802.
[6] Y. Pommier, A. A. Johnson, C. Marchand, *Nat. Rev. Drug Discovery* **2005**, *4*, 236 – 248.
[7] D. J. Hazuda, P. Felock, M. Witmer, A. Wolfe, K. Stillmock, J. A. Grobler, A. Espeseth, L. Gabryelski, W. Schleif, C. Blau, M. D. Miller, *Science* **2000**, *287*, 646 – 650.
[8] D. J. Hazuda, S. D. Young, J. P. Guare, N. J. Anthony, R. P. Gomez, J. S. Wai, J. P. Vacca, L. Handt, S. L. Motzel, H. J. Klein, G. Dornadula, R. M. Danovich, M. V. Witmer, K. A. Wilson, L. Tussey, W. A. Schleif, L. S. Gabryel-

ski, L. Jin, M. D. Miller, D. R. Casimiro, E. A. Emini, J. W. Shiver, *Science* **2004**, *305*, 528 – 532.
[9] T. S. Yoshinaga, A. Fujishita, T. Fujiwara in *9th Conference on Retroviruses and Opportunistic Infections*, Seattle, WA, USA, **2002**.
[10] S. Young in *The XIV International AIDS Conference*, Barcelona, Spain, **2002**.
[11] N. Neamati, *Expert Opin. Invest. Drugs* **2001**, *10*, 281 – 296.
[12] Y. Goldgur, R. Craigie, G. H. Cohen, T. Fujiwara, T. Yoshinaga, T. Fujishita, H. Sugimoto, T. Endo, H. Murai, D. R. Davies, *Proc. Natl. Acad. Sci. USA* **1999**, *96*, 13 040 – 13 043.
[13] M. C. Nicklaus, N. Neamati, H. Hong, A. Mazumder, S. Sunder, J. Chen, G. W. Milne, Y. Pommier, *J. Med. Chem.* **1997**, *40*, 920 – 929.
[14] N. Neamati, H. Hong, S. Sunder, G. W. Milne, Y. Pommier, *Mol. Pharmacol.* **1997**, *52*, 1041 – 1055.
[15] N. Neamati, H. Hong, A. Mazumder, S. Wang, S. Sunder, M. C. Nicklaus, G. W. Milne, B. Proksa, Y. Pommier, *J. Med. Chem.* **1997**, *40*, 942 – 951.
[16] H. Hong, N. Neamati, S. Wang, M. C. Nicklaus, A. Mazumder, H. Zhao, T. R. Burke, Jr., Y. Pommier, G. W. Milne, *J. Med. Chem.* **1997**, *40*, 930 – 936.
[17] M. L. Barreca, A. Rao, L. De Luca, M. Zappala, C. Gurnari, P. Monforte, E. De Clercq, B. Van Maele, Z. Debyser, M. Witvrouw, J. M. Briggs, A. Chimirri, *J. Chem. Inf. Comput. Sci.* **2004**, *44*, 1450 – 1455.
[18] R. Dayam, T. Sanchez, O. Clement, R. Shoemaker, S. Sei, N. Neamati, *J. Med. Chem.* **2005**, *48*, 111 – 120.
[19] H. A. Carlson, K. M. Masukawa, K. Rubins, F. D. Bushman, W. L. Jorgensen, R. D. Lins, J. M. Briggs, J. A. McCammon, *J. Med. Chem.* **2000**, *43*, 2100 – 2114.
[20] J. Deng, K. W. Lee, T. Sanchez, M. Cui, N. Neamati, J. M. Briggs, *J. Med. Chem.* **2005**, *48*, 1496 – 1505.
[21] D. M. Karussis, D. Lehmann, S. Slavin, U. Vourka-Karussis, R. Mizrachi-Koll, H. Ovadia, T. Kalland, O. Abramsky, *Proc. Natl. Acad. Sci. USA* **1993**, *90*, 6400 – 6404.
[22] M. Bengtsson, B. Simonsson, K. Carlsson, B. Nilsson, B. Smedmyr, B. Termander, G. Oberg, T. H. Totterman, *Transplantation* **1992**, *53*, 882 – 888.
[23] G. del Real, M. Llorente, L. Bosca, S. Hortelano, A. Serrano, P. Lucas, L. Gomez, J. L. Toran, C. Redondo, C. Martinez, *Aids* **1998**, *12*, 865 – 872.
[24] S. Jonsson, G. Andersson, T. Fex, T. Fristedt, G. Hedlund, K. Jansson, L. Abramo, I. Fritzson, O. Pekarski, A. Runstrom, H. Sandin, I. Thuvesson, A. Bjork, *J. Med. Chem.* **2004**, *47*, 2075 – 2088.
[25] C. A. Lipinski, *J. Pharmacol. Toxicol. Methods* **2000**, *44*, 235 – 249.
[26] C. A. Lipinski, F. Lombardo, B. W. Dominy, P. J. Feeney, *Adv. Drug Delivery Rev.* **2001**, *46*, 3 – 26.
[27] C. Plasencia, R. Dayam, Q. Wang, J. Pinski, T. R. Burke, Jr., D. I. Quinn, N. Neamati, *Mol. Cancer Ther.* **2005**, *4*, 1105 – 1113.
[28] K. Palm, P. Stenberg, K. Luthman, P. Artursson, *Pharm. Res.* **1997**, *14*, 568 – 571.
[29] J. Kelder, P. D. Grootenhuis, D. M. Bayada, L. P. Delbressine, J. P. Ploemen, *Pharm. Res.* **1999**, *16*, 1514 – 1519.
[30] W. J. Egan, W. P. Walters, M. A. Murcko, *Curr. Opin. Drug Discovery Dev.* **2002**, *5*, 540 – 549.
[31] W. J. Egan, G. Lauri, *Adv. Drug Delivery Rev.* **2002**, *54*, 273 – 289.
[32] Y. Goldgur, F. Dyda, A. B. Hickman, T. M. Jenkins, R. Craigie, D. R. Davies, *Proc. Natl. Acad. Sci. USA* **1998**, *95*, 9150 – 9154.
[33] Insight II, Accelrys, Inc., San Diego, CA, USA, **2002**.
[34] GOLD version 1.2, CCDC, Cambridge, UK.
[35] G. Jones, P. Willett, R. C. Glen, A. R. Leach, R. Taylor, *J. Mol. Biol.* **1997**, *267*, 727 – 748.
[36] J. W. Nissink, C. Murray, M. Hartshorn, M. L. Verdonk, J. C. Cole, R. Taylor, *Proteins Struct. Funct. Genet.* **2002**, *49*, 457 – 471.

Received: August 3, 2005
Revised: October 9, 2005
Published online on December 20, 2005

